

Topological production of charmonia with event-shape engineering in pp collisions at $\sqrt{s} = 13$ TeV using PYTHIA8

Aswathy Menon Kavumpadikkal Radhakrishnan^{1,*}, Suraj Prasad^{1,†}, Neelkamal Mallick^{1,2,‡} and Raghunath Sahoo^{1§}

¹*Department of Physics, Indian Institute of Technology Indore, Simrol, Indore 453552, India and*

²*University of Jyväskylä, Department of Physics, P.O. Box 35, FI-40014, Jyväskylä, Finland*

(Dated: December 1, 2025)

The production of heavy quarks (charm and beauty) in high-energy hadronic and nuclear collisions provides an excellent testing ground for the theory of strong interaction and validates models based on quantum chromodynamics. In this work, prompt and nonprompt production of J/ψ in pp collisions at $\sqrt{s} = 13$ TeV are studied as a function of transverse sphericity using PYTHIA8. J/ψ is reconstructed via its electromagnetic decay to dielectrons and dimuons, in mid- and forward-rapidity, respectively. Transverse sphericity, an event shape observable, is used to distinguish hard QCD events from the softer, isotropic ones. In PYTHIA8, the production of J/ψ can be influenced by the average number of multiple parton interactions ($\langle N_{\text{mpi}} \rangle$), owing to the underlying events (UE), which have a dominant contribution to particle production at lower transverse momentum. Since transverse sphericity is correlated to $\langle N_{\text{mpi}} \rangle$, this can serve as an experimentally available tool for event selection to study the underlying QCD processes influencing the prompt and nonprompt J/ψ production. This study reveals the correlation between heavy-flavor production dynamics and topological event selection in pp collisions using PYTHIA8, whose relevance awaits experimental validation.

I. INTRODUCTION

Experimental explorations at the world’s most powerful particle accelerator facilities like the Large Hadron Collider (LHC) at CERN, Switzerland, and the Relativistic Heavy Ion Collider (RHIC) at BNL, USA aim to study the formation of a deconfined state of hot and dense sub-nuclear matter, called as Quark-Gluon Plasma (QGP), and also to understand the fundamental processes of “hadronization”, which explain the formation of hadrons out of quarks [1]. During such violent collisions of nuclear matter, quarks and gluons are liberated as the relevant degrees of freedom for a very short duration ($\simeq 10^{-23}$ s). In this environment, heavy quarks (charm and beauty) are produced predominantly in the initial hard-partonic interactions, which can be reliably understood via perturbative quantum chromodynamics (pQCD). As heavy quarks are created early in the collision, their production provides an excellent testing ground for the theory of strong interaction *i.e.* QCD. Within the framework of the QCD factorization theorem, the heavy quark production cross-section is expressed as the convolution of three terms: (i) the parton distribution functions (PDFs), (ii) the parton hard-scattering cross sections, and (iii) the heavy-flavor fragmentation functions [2].

Among the various hadrons containing heavy quarks, quarkonia—bound states of a heavy quark and its antiquark—have been studied extensively, with particular emphasis on the lightest charmonium vector meson, J/ψ . This is because although the initial produc-

tion of $c\bar{c}$ pairs from hard-partonic interactions is fairly described by pQCD, the subsequent formation of a color-neutral bound state involves soft-scale, non-perturbative processes that are still not fully understood and are typically addressed via phenomenological models [3].

The inclusive J/ψ production occurs via two distinct mechanisms, *i.e.* prompt and non-prompt. Prompt J/ψ are produced directly in the hard scattering or formed from the radiative decay of higher charmonium states. They reflect the early collision dynamics and serve as ideal tools to test strong-interaction models and study suppression/regeneration in the QGP. In contrast, non-prompt J/ψ are the weak decay products of beauty hadrons [4–6], which carry most of the momentum of their parent hadrons, thus providing insight into beauty production in elementary, hadronic, and heavy-ion collisions. Together, they offer complementary probes of quarkonium production mechanisms. These two production modes exhibit distinctive topological signatures: the decay vertex of non-prompt J/ψ is significantly displaced from the primary vertex compared to prompt J/ψ because of the longer lifetime of the weakly decaying parent beauty hadrons [7, 8]. Exploiting these features allows experimental separation of prompt and non-prompt contributions, which in turn provides crucial insights into hadronization mechanisms in both the charm and beauty sectors.

In experiments, the inclusive J/ψ measurements are performed by reconstructing J/ψ through its electromagnetic decays to dileptons, as the hadronic decays are mostly suppressed, which is described by the Okubo-Zweig-Iizuka (OZI) rule. Among the experiments at the LHC, ALICE is capable of measuring the topological productions of J/ψ at both midrapidity and forward rapidity regions. The production of J/ψ at midrapidity ($|y| < 0.9$) is measured via the dielectron

* Aswathy.Menon@cern.ch

† Suraj.Prasad@cern.ch

‡ Neelkamal.Mallick@cern.ch

§ Corresponding author: Raghunath.Sahoo@cern.ch

decay channel *i.e.* $J/\psi \rightarrow e^+ + e^-$. In contrast, the production at the forward rapidity ($2.5 < y < 4$) is performed via dimuon decay channel *i.e.* $J/\psi \rightarrow \mu^+ + \mu^-$.

In Refs. [9–12], the ALICE Collaboration explores the production of self-normalized yield of inclusive J/ψ , as a function of self-normalized charged particle density at midrapidity for event selection based on multiplicity at both mid-rapidity and forward rapidity regions. Here, the collision energy dependence of the self-normalized yield of J/ψ is also explored. Such correlation studies of charmonium production with charged particle multiplicity (N_{ch}) are important to explore the interplay between hard and soft mechanisms of J/ψ production, both at the partonic level and at hadronization [13]. One observes that the self-normalized yield of J/ψ at forward rapidity increases linearly as a function of self-normalized charged particle density at midrapidity when event classification is performed based on multiplicity at midrapidity in pp collisions at $\sqrt{s} = 5.02$ TeV. This follows the $x = y$ line. However, the self-normalized yield of J/ψ starts to deviate from the linear behaviour with an increase in \sqrt{s} . The deviations from the linear behaviour become stronger when the measurement of J/ψ is changed from forward rapidity to midrapidity regions, irrespective of event classification based on midrapidity or forward rapidity multiplicity [10]. This observation underlines the fact that the production of J/ψ is strongly affected when one moves from the midrapidity to forward rapidity regions. The phenomenological studies suggest that this non-linear behaviour is partially contributed from the non-prompt production of J/ψ [13]. In addition, the latest ALICE experimental data on the multiplicity-dependence of J/ψ where both N_{ch} and J/ψ yields are measured at forward rapidities, reiterate the finding of the steeper-than-linear increase of their correlation, attributing it to the autocorrelation effects [12]. Thus, it is necessary to make a systematic study of the prompt and non-prompt production of J/ψ as a function of pseudo-rapidity.

The pQCD-based event generators, such as PYTHIA8, are able to explain the heavy-flavour production up to a greater extent, in addition to a number of heavy-ion-like observations in high multiplicity pp collisions [8, 14–16]. This is possible thanks to the improved implementation of multipartonic interactions (MPI), color reconnection (CR), and rope hadronisation (RH) [14, 15]. The strange and multi-strange hadron ratios showing strangeness enhancement, as well as the particle ratios carrying information about the radial flow, are well explained by PYTHIA8 with MPI, CR, and RH [14, 15, 17]. Even the increase in charmonium production with charged-particle multiplicity is well explained by PYTHIA8 when MPI is included [18–20]. In fact, it is identified that the J/ψ production in pp collisions is either directly linked to a strong hadronic activity, which increases particle production and biases the $dN_{\text{ch}}/d\eta$ distributions to higher values, or the scenario is that the influence of MPI extends to the domain of hard processes, affecting the harder

momentum scales relevant for quarkonia production [9]. Moreover, the production of high-momentum and heavier particles in the initial scattering restricts the energy available for MPI and, in turn, affects the particle produced through MPI and the event shape. However, estimating the number of MPI (N_{mpi}) in experiments is not trivial. This challenge could be overcome if event-shape observables proportional to N_{mpi} are employed, one such event classifier being the transverse sphericity, S_0 [14]. In this context, the present work bridges this gap by utilising an event-shape-based approach—through transverse sphericity—to investigate the dynamics of J/ψ production.

S_0 enables us to segregate hard jetty-like events from soft-processes dominated isotropic events based on the geometry of particle production in each event, the classification strength of which is retained from pp to Pb-Pb collisions [21–26]. Interestingly, the classification strength of transverse sphericity changes weakly with a change in rapidity [27], which makes transverse sphericity a suitable event classifier to study the production of prompt and non-prompt J/ψ in midrapidity and forward rapidity regions. Moreover, in addition to multiplicity-based studies, classifying collisions based on S_0 gives us the added benefit of analysing various mechanisms of particle production or hadronization for charm and beauty quarks [28]. Thus, this paper explores the transverse sphericity and multiplicity-dependent production of prompt and non-prompt J/ψ at midrapidity and forward rapidity regions in pp collisions at $\sqrt{s} = 13$ TeV using PYTHIA8 through several observables believed to be sensitive to the underlying production mechanisms and autocorrelation bias effects. J/ψ production is studied via the electronic decay channel at midrapidity and the muonic decay channel at the forward rapidity regions. We focus on the observables such as partonic modification factor Q_{pp} , mean transverse momentum $\langle p_T \rangle$, non-prompt J/ψ fraction f_B , and self-normalized yield of prompt and non-prompt J/ψ .

The paper is organised as follows. In Section I, we provide a brief introduction and motivation for the study. Section II discusses the event generation and methodology. In Section III, we present our results and discuss the same. Finally, findings of the paper are summarised in Section IV, with a brief future outlook.

II. EVENT GENERATION AND METHODOLOGY

In this section, we briefly discuss the event generation using PYTHIA8, along with the tunes used in this study. A brief discussion on the event-shape selection using transverse sphericity is also made.

A. PYTHIA8

The pQCD-based Monte Carlo event generators such as PYTHIA8 describe many features of relativistic pp collisions at the RHIC and LHC energies. PYTHIA8 has several models which incorporate soft and hard partonic interactions, initial and final state parton showers, multiple-partonic interactions (MPI), beam remnants, string fragmentation, and hadronic decays [29, 30]. Here, along with MPI-based interactions, $2 \rightarrow 2$ hard processes are implemented, which leads to the production of charm and beauty hadrons. In this study, we have used the 4C-tune of PYTHIA8 [31] (version 8.308) to generate the minimum bias pp collisions at $\sqrt{s} = 13$ TeV, which include the inelastic and non-diffractive components (HardQCD:all = on) of the total collision cross section. In addition, a p_T cut-off of $p_T > 0.5$ GeV/c (using PhaseSpace:pTHatMinDiverge) is set to avoid the divergence of QCD processes in the limit $p_T \rightarrow 0$. Along with the color reconnection (CR) and MPI, we have enabled all possible charmonia and bottomonia production processes available in PYTHIA using “Charmonium:all=on” and “Bottomonium:all=on”. J/ψ is allowed to decay into opposite charge pairs of electrons and muons individually to have better statistics. For both electronic and muonic decay channels of J/ψ , we produce 10 billion minimum bias events with the tunes mentioned above in pp collisions at $\sqrt{s} = 13$ TeV. A detailed description of event generation, along with identification of prompt and non-prompt J/ψ , can be found in Ref. [8].

In PYTHIA8, the production of heavy quark (Q) and anti-quark (\bar{Q}) pairs is implemented through the pQCD scattering processes which include the pair creation through gluon fusion ($gg \rightarrow Q\bar{Q}$) and light quark (q) anti-quark (\bar{q}) pair annihilation ($q\bar{q} \rightarrow Q\bar{Q}$) [13]. In addition to this, the production of heavy quarks can be possible through the gluon splitting of parton showers, i.e., $g \rightarrow Q\bar{Q}$. At sufficiently large energy transfer, the heavy quarks also contribute to the parton distribution function, leading to the production of heavy quarks via flavour excitation ($gQ \rightarrow gQ$). Similarly, the quarkonia ($c\bar{c}$ or $b\bar{b}$) production in PYTHIA8 can also be implemented via several mechanisms. The leading order NRQCD channels of $Q\bar{Q}$ production via color-singlet and color-octet pre-resonant states are included in the pQCD processes. The cluster collapse mechanism also contributes to quarkonia production when a heavy quark gets connected to a corresponding heavy antiquark close in phase space to form a quarkonium bound state, during the hadronization stage. If charmonia ($c\bar{c}$) is produced from the weak decay of a beauty hadron, it is referred to as non-prompt charmonium production.

B. Transverse sphericity

Transverse sphericity (S_0) is an event shape observable that potentially characterizes the geometry of an

event based on the azimuthal distribution of the particles produced. It is defined for a unit vector $\hat{n}(n_T, 0)$ in the transverse plane, which minimises the sum of cross-products in the bracket as shown below [14, 17, 32]:

$$S_0 = \frac{\pi^2}{4} \min_{\hat{n}} \left(\frac{\sum_{i=1}^{N_{\text{ch}}} |\vec{p}_{T_i} \times \hat{n}|}{\sum_{i=1}^{N_{\text{ch}}} |\vec{p}_{T_i}|} \right)^2 \quad (1)$$

Here, \vec{p}_{T_i} stands for the transverse momentum vector of i^{th} charged particle, in an event and the iteration to find the suitable \hat{n} runs over all charged particles (N_{ch}). The multiplication factor $\pi^2/4$ in Eq. (1) is to normalize the quantity S_0 to lie between 0 and 1. Only the charged tracks within $|\eta| < 0.8$ with $p_T > 0.15$ GeV/c are considered for the calculation of S_0 . In this study, S_0 is constructed by setting $|\vec{p}_{T_i}| = 1.0$ to reduce the charge-to-neutral bias, where a minimum constraint of 10 charged particles at $|\eta| < 0.8$ and $p_T > 0.15$ GeV/c is applied for each collision so that the description of unweighted sphericity is meaningful [17]. The lower limit, $S_0 \rightarrow 0$, corresponds to jetty events containing back-to-back jets, which are consequences of hard scatterings. On the other hand, $S_0 \rightarrow 1$ depicts isotropic events where particles are produced uniformly in the azimuthal plane, resulting from softer interactions. Thus, qualitatively, transverse sphericity S_0 disentangles pQCD-dominated hard processes from soft-QCD processes, helping in understanding the underlying particle production mechanism. Here, 20% of events having the lowest and highest values of S_0 are respectively referred to as jetty and isotropic events. The cuts in S_0 for jetty and isotropic events for various V0M multiplicity classes are shown in Tab. I. A comparison of the sphericity distribution from PYTHIA8 results to that of the experimental data from the ALICE collaboration for the highest V0M multiplicity class (0–1%) is presented in Fig. 7 (Appendix 1), where a good qualitative and quantitative similarity is observed between the two.

V0M Percentile	$\langle dN_{\text{ch}}/d\eta \rangle_{ \eta < 0.5}$	S_0 range	
		Jetty	Isotropic
0 – 1	20.17	0–0.646	0.844–1
1 – 5	12.47	0–0.576	0.812–1
5 – 10	7.81	0–0.528	0.784–1
10 – 20	5.27	0–0.504	0.770–1
20 – 40	3.34	0–0.486	0.760–1
40 – 100	2.39	0–0.468	0.750–1
0 – 100	3.74	0–0.525	0.785–1

TABLE I. Transverse sphericity cuts for the jetty and isotropic events for different multiplicity classes in pp collisions at $\sqrt{s} = 13$ TeV using PYTHIA8. The errors for the mean charged particle multiplicity density are too small ($< 1\%$), hence not tabulated.

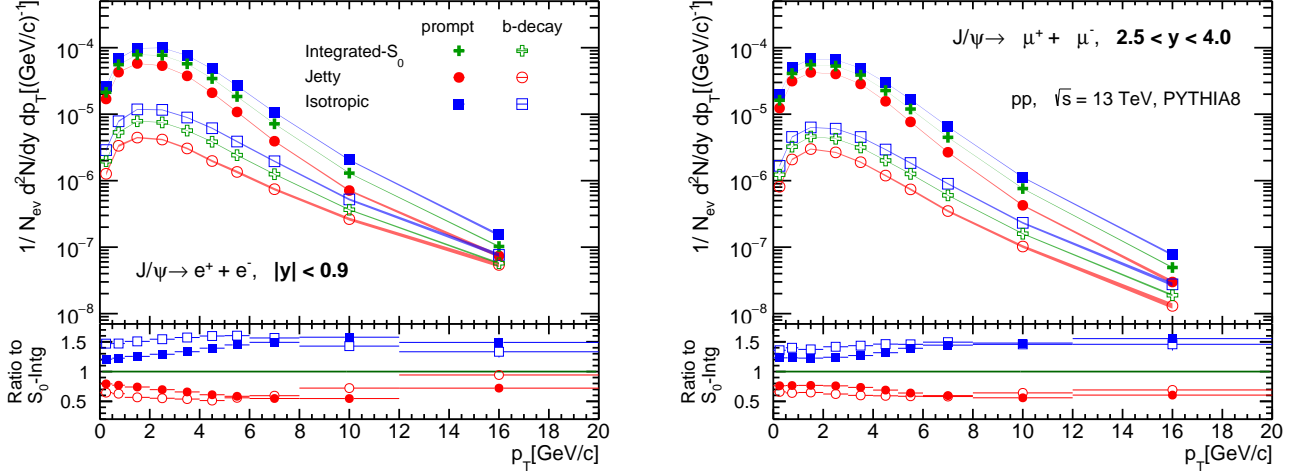


FIG. 1. (Color online) Event-normalized transverse momentum (p_T) spectra of prompt and non-prompt J/ψ in S_0 -integrated, jetty and isotropic events from pp collisions at $\sqrt{s} = 13$ TeV using PYTHIA8, for dielectron (left) and dimuon (right) production channels at $|y| < 0.9$ and $2.5 < y < 4.0$ rapidity ranges respectively for (0–100%) V0M class. The ratio of p_T spectra of the jetty and isotropic to S_0 -integrated events is shown in the bottom panel.

III. RESULTS AND DISCUSSIONS

This section explains the results we obtained, as a function of transverse sphericity (S_0) for prompt and non-prompt J/ψ produced in pp collisions at $\sqrt{s} = 13$ TeV using PYTHIA8. Here, J/ψ is reconstructed via the dileptonic decay channels $J/\psi \rightarrow e^+ + e^-$ at midrapidity ($|y| < 0.9$) and $J/\psi \rightarrow \mu^+ + \mu^-$ in the forward rapidity ($2.5 < y < 4$). From this point onwards, J/ψ in the mid-rapidity and forward rapidity respectively implies the reconstruction using $J/\psi \rightarrow e^+ + e^-$ channel and $J/\psi \rightarrow \mu^+ + \mu^-$ channel.

Shown in Fig. 1 are the S_0 dependence of event-normalized p_T spectra of prompt and non-prompt J/ψ produced in pp collisions simulated using PYTHIA8 at $\sqrt{s} = 13$ TeV for (0–100%) V0M class. The p_T spectra of J/ψ , reconstructed via dielectron and dimuon channels, are shown in the left and right plots of Fig. 1, respectively. We observe that the yield of non-prompt J/ψ is almost ten times smaller than that of prompt J/ψ in the low p_T regime while this difference shrinks as we approach higher values of p_T for both the rapidity regions. Towards the low- p_T region, the contributions of prompt J/ψ come primarily from the charmonia produced in the leading order semi-hard processes, i.e., $q\bar{q} \rightarrow C$ and $gg \rightarrow C$. Here, the probability of beauty hadron production is significantly small due to its large mass compared to charmonium states. Further, in Ref. [13], the authors show that at high p_T -regime, the particle production is largely dominated by the hard scatterings, where the production of beauty hadrons is comparable to charmonium states. Thus, the hardening of p_T -spectrum of non-prompt J/ψ as compared to prompt J/ψ is a consequence of the competing effects

of two different production mechanisms of charmonium states and beauty hadrons in different regions of transverse momentum. We note that these trends are in line with the results obtained from the experiments [33–35].

We also see a considerable dependence of transverse sphericity on the p_T -dependent yield of topological production of J/ψ in both the rapidity regions, as shown in Fig. 1. Here, the production of both prompt and non-prompt J/ψ is observed to be favoured more in isotropic events as compared to the jetty events. In Refs. [14, 15, 27], it is explored that the transverse sphericity possesses a large correlation with N_{mpi} . Additionally, it is also concluded in Ref. [20] that the production of inclusive J/ψ , which are mostly prompt in nature, is favored in events having large N_{mpi} . In fact, the yield of inclusive J/ψ increases linearly with N_{mpi} [20]. The observation of a higher (lower) prompt J/ψ yield in isotropic (jetty) events, which corresponds to events having large (small) N_{mpi} as compared to S_0 -integrated events, is a testimony of the observations shown in Ref. [20]. Analogously, it can also be argued that the events having large N_{mpi} favor the b-hadron production, as compared to events having small N_{mpi} , which results in a larger yield of non-prompt J/ψ for isotropic events, as compared to the jetty events [13].

A clearer comparison of yields between different S_0 classes is presented in the bottom panel of Fig. 1, where the ratio of p_T spectra for isotropic and jetty events to that of the S_0 -integrated events are shown for both prompt and non-prompt J/ψ . One can see that the relative prompt J/ψ production in isotropic events increases with p_T till 10 GeV/c to fall gradually thereafter, indicating the hardness of p_T -spectra of prompt J/ψ in isotropic events in comparison to S_0 -integrated events. In contrast, it decreases with p_T for jetty events to rise

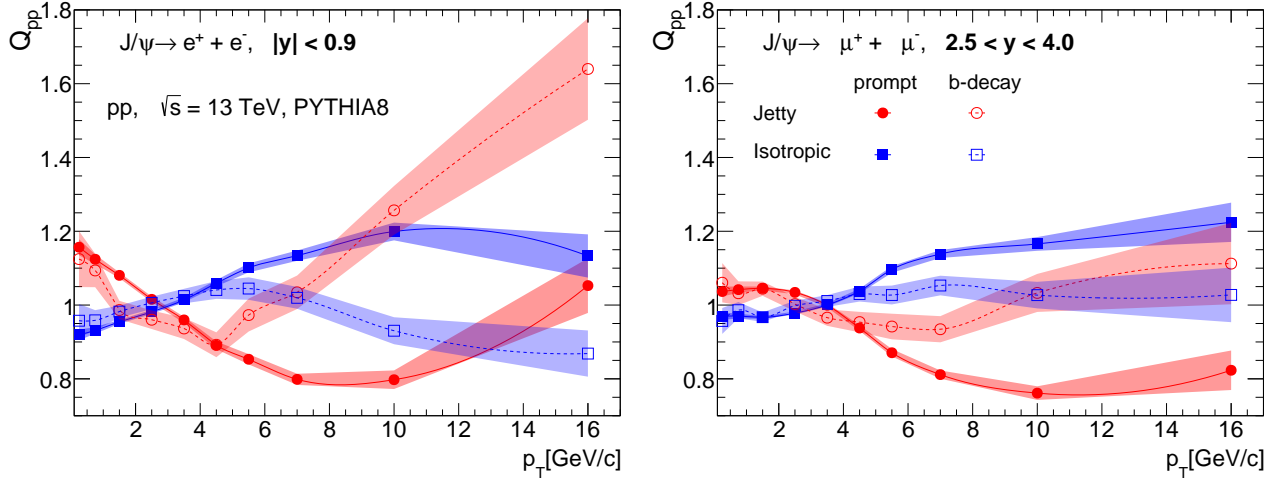


FIG. 2. (Color online) Q_{pp} as a function of p_T for prompt and non-prompt J/ψ in mid (left) and forward (right) rapidities for jetty and isotropic events in pp collisions at $\sqrt{s} = 13$ TeV using PYTHIA8.

after $p_T \approx 10$ GeV/ c , showing the softness of p_T -spectra in jetty events as compared to S_0 -integrated events. In Ref. [13], the authors show that a non-negligible amount of prompt J/ψ are formed through the cluster collapse mechanism, which is largely enhanced for the CR-on scenario for the events with large N_{mpi} . Thus, the hardness and softness of p_T -spectra for the isotropic and jetty events, respectively, for the prompt J/ψ case are a consequence of effects from colour reconnection, where the charm quarks from independent partonic scatterings combine to form charmonium states having a large transverse momentum. The effect of colour reconnection is enhanced for the events having large N_{mpi} , consequently, the isotropic event, leading to the observed hardening of prompt J/ψ spectra. At the same time, the yield in both isotropic and jetty events relative to S_0 -integrated events of non-prompt J/ψ shows only minute dependence on p_T till $p_T \approx 6$ GeV/ c in both isotropic and jetty events. However, after $p_T > 6$ GeV/ c , the relative non-prompt J/ψ production abruptly decreases for isotropic events and steeply increases for jetty events to converge with the S_0 -integrated yield. The smaller hardening of non-prompt J/ψ spectra as compared to the prompt case is because of the large mass of the beauty hadrons, which are produced in the initial hard scatterings, which remain unaffected by CR [20]. The effects of hardening (and softening) of p_T -spectra of prompt and non-prompt J/ψ are diminished at the forward rapidity regions because the effects of MPI are found to be smaller when observations are made in forward rapidity regions, as compared to mid-rapidity, where the particle yield is significantly higher [27].

In experiments, it is observed that the self-normalized yield of charged particles for $p_T > 4$ GeV/ c shows a stronger than linear increase with an increase in charged particle multiplicity density in the midrapidity region [28]. These observations are also made for

strange [36] and charm [9–12, 37, 38] hadrons at high- p_T regions. With PYTHIA8, the stronger-than-linear increase of the self-normalized particle yield of prompt and non-prompt J/ψ is shown in Fig. 5, the discussion of which will follow later. As discussed, these effects mostly come as a consequence of autocorrelation bias. Also, event classifiers based on multiplicity can lead to contributions from multi-jet scatterings in the final state [39, 40]. On the other hand, event classifiers based on event shapes, such as transverse sphericity, can probe N_{mpi} , and the contributions from multi-jet topologies can be effectively reduced. Since these effects have p_T dependence, one needs to make a comparison of transverse momentum spectra by taking out the contributions from the final state multiplicity.

To exclusively understand the modification in the p_T spectral shape for prompt and non-prompt J/ψ for isotropic and jetty events, we study the partonic modification factor Q_{pp} whose formulation is inspired by the nuclear modification factor, R_{AA} . Through Q_{pp} , we aim to make a qualitative comparison of the event-normalized p_T -differential yield of prompt and non-prompt J/ψ from the isotropic and jetty events to that of S_0 -integrated events, where the yield is scaled by the average number of prompt (or non-prompt) J/ψ in that particular sphericity class. Consequently, Q_{pp} is defined as follows [27, 41].

$$Q_{pp} = \frac{d^2 N_{J/\psi}^{S_0} / \langle N_{J/\psi}^{S_0} \rangle dy dp_T}{d^2 N_{J/\psi}^{S_0-int} / \langle N_{J/\psi}^{S_0-int} \rangle dy dp_T} \quad (2)$$

Here, $\langle N_{J/\psi}^{S_0} \rangle$ and $\langle N_{J/\psi}^{S_0-int} \rangle$ are the average number of prompt or non-prompt J/ψ in corresponding sphericity event class and S_0 -integrated events, respectively.

Figure 2 shows the transverse momentum dependence of the partonic modification factor defined in Eq. (2) for prompt and non-prompt J/ψ . The left and the right panels show the results for the prompt and non-prompt J/ψ ,

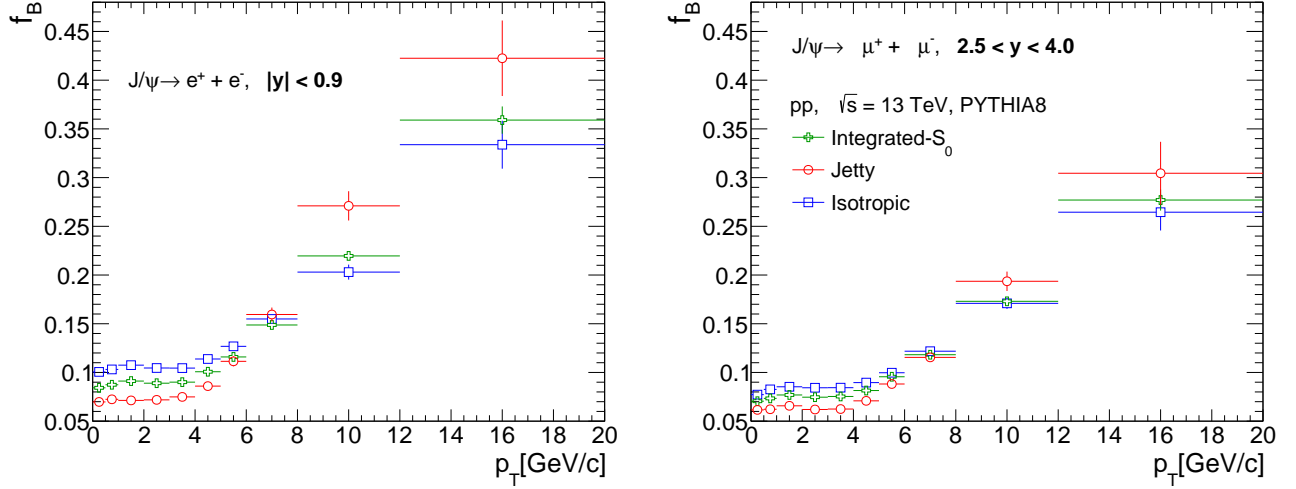


FIG. 3. (Color online) The fraction of non-prompt J/ψ produced as a function of p_T in midrapidity (left) and forward rapidity (right) for S_0 -integrated, jetty and isotropic events from pp collisions at $\sqrt{s} = 13$ TeV using PYTHIA8

at mid and forward rapidity regions, respectively. At the mid-rapidity, the trend for both prompt and non-prompt J/ψ is such that it first increases (decreases) with an increase in p_T for the isotropic (jetty) case and then starts to fall (rise) towards higher p_T . However, Q_{pp} attains the peak (valley) at a much earlier p_T (~ 5 GeV/c) in the case of non-prompt J/ψ than for the prompt J/ψ . As discussed earlier, both prompt and non-prompt J/ψ p_T spectra show different levels of hardening for different classes of sphericity, which is reflected in the positions of peaks and valleys in the Q_{pp} spectra of prompt and non-prompt J/ψ . Further, the observed deviations from unity at high- p_T for the non-prompt J/ψ measured at the midrapidity region for both the isotropic and jetty events are interesting. The beauty hadron production is often accompanied by a high-energy jet in the opposite direction, which makes the events pencil-like. On the contrary, when the events are isotropic, which corresponds to a high N_{mpi} , most of the energy is used up in particle production as no beauty hadrons are produced in the initial scatterings [13]. This shows that the events where the beauty hadrons are produced acquire a unique shape, which is picked up by transverse sphericity. In addition, small auto-correlation bias effects may contribute here as $S_0 \propto N_{ch}$, which can be avoided when measurements are done at different rapidity regions.

The measurements made at forward rapidity (right plot) are crucial, as negligible autocorrelation bias is expected. Here, Q_{pp} vary smoothly with increase in p_T . Q_{pp} , which starts slightly above (below) 1 for jetty (isotropic) events at low p_T , suddenly starts to decrease (increase) after 3 GeV/c for both prompt and non-prompt J/ψ . Q_{pp} from isotropic and jetty events has its first crossing at around 3-4 GeV/c for both prompt and non-prompt J/ψ and the second crossing at ~ 10 GeV/c for the non-prompt J/ψ case. However, unlike in midrapidity, here at forward rapidity, the non-prompt

J/ψ shows no deviations from unity. This is a testimony that the production of beauty hadrons at forward rapidity would not modify the event shape measured through the charged particles in the midrapidity region.

To understand the contribution of J/ψ produced from the decay of b -hadrons to the inclusive J/ψ production, the fraction of non-prompt to inclusive J/ψ (f_B) is studied as a function of transverse momentum and transverse sphericity in (0-100%) V0M class, both at midrapidity and forward rapidity regions, as shown in Fig. 3. A qualitative similarity of our results with the ALICE and LHCb data could be observed from the comparison presented in Fig. 8 in the Appendix 1. Similar to the experimental observations at midrapidity in Ref. [33], the non-prompt J/ψ fraction stays independent of p_T for $p_T \leq 4$ GeV/c after which f_B increases steadily with an increase in p_T . This relative increase in the number of non-prompt J/ψ to inclusive J/ψ with an increase in p_T is consistent with the observations of hardening of non-prompt J/ψ p_T -spectra with respect to prompt J/ψ , as shown in Fig. 1, for both the rapidity regions. In addition, f_B shows significant transverse sphericity dependence. Here, at the midrapidity region, for $p_T \leq 6$ GeV/c, isotropic events show a larger value of f_B . Interestingly, this trend is reversed for $p_T > 6$ GeV/c, where jetty events lead f_B . This transverse sphericity dependence at the low p_T region reflects the effects of MPI on the production of beauty hadrons. Here, a larger fraction of non-prompt J/ψ is produced in the isotropic events (large N_{mpi}) as compared to the jetty events (having small N_{mpi}). This is a testimony that, in PYTHIA8, MPI activity can affect the beauty hadron production [13]. However, at high p_T regions, a large fraction of beauty hadrons are produced from initial hard scattering. These hard scatterings are significantly large in jetty events, which leads to the enhanced value of f_B at large values of p_T . A similar observation is also made at the forward rapidity region. Here,

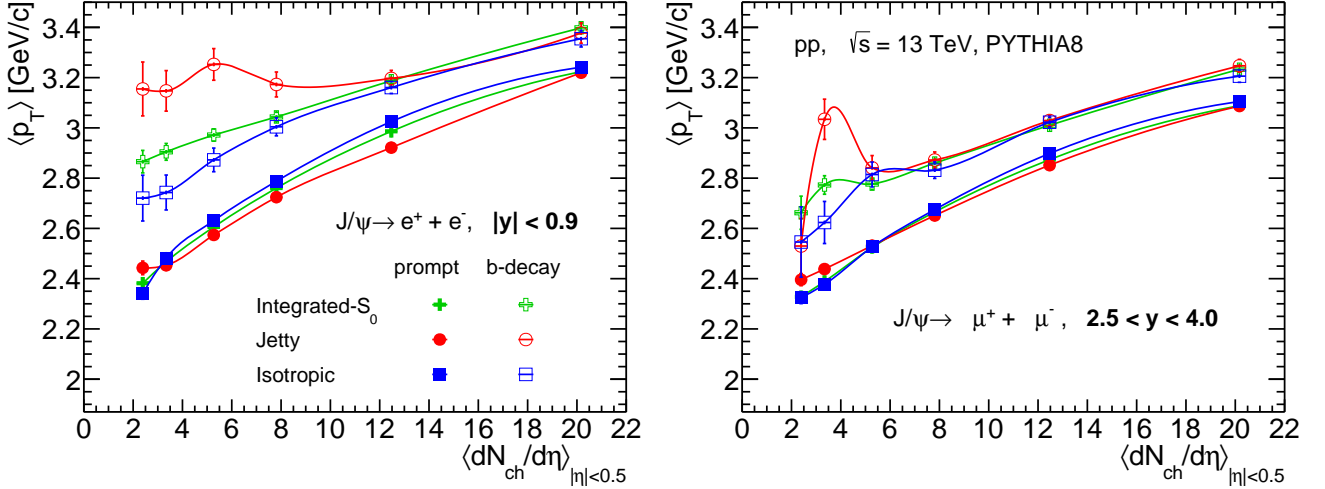


FIG. 4. (Color online) Mean transverse momentum ($\langle p_T \rangle$) as a function of midrapidity charged particle multiplicity density for prompt and non-prompt J/ψ in mid (left) and forward (right) rapidity regions for S_0 -integrated, jetty and isotropic events for pp collisions at $\sqrt{s} = 13$ TeV using PYTHIA8

however, the crossing of f_B for jetty and isotropic events happens at $p_T \approx 8$ GeV/c. In addition, we find f_B to be smaller in forward rapidity as compared to the midrapidity region, for all S_0 classes.

Figure 4 shows the mean transverse momentum ($\langle p_T \rangle$) as a function of average charged particle multiplicity at midrapidity ($\langle dN_{ch}/d\eta \rangle_{|\eta|<0.5}$) for prompt and non-prompt J/ψ in the three S_0 classes for measurements at mid rapidity (left plot) and forward rapidity (right plot) in pp collisions at $\sqrt{s} = 13$ TeV using PYTHIA8. $\langle p_T \rangle$ of both prompt and non-prompt J/ψ is seen to rise with multiplicity, where midrapidity measurements achieve greater magnitudes of $\langle p_T \rangle$ than those in forward rapidity. This observation of rapidity dependence of $\langle p_T \rangle$ is consistent with the results of light flavour hadrons, as shown in Ref. [27]. For both the pseudorapidity regions, one finds a larger $\langle p_T \rangle$ for the non-prompt J/ψ as compared to the prompt case. Since the non-prompt J/ψ carries most of the transverse momentum of its parent beauty hadrons, $\langle p_T \rangle$ of non-prompt J/ψ is the reflection of $\langle p_T \rangle$ of the decaying beauty hadrons, which is evidently larger than the $\langle p_T \rangle$ of prompt J/ψ . This is because the beauty hadrons that contribute to non-prompt J/ψ possess a larger mass compared to the charmonium states. In other words, Fig. 4 reflects the mass ordering of $\langle p_T \rangle$, which is consistent with the mass-ordering of $\langle p_T \rangle$ for different hadrons in the light-flavour sector [42]. There is also a notable S_0 dependence for the enhancement of $\langle p_T \rangle$ with increase in $\langle dN_{ch}/d\eta \rangle_{|\eta|<0.5}$, especially for the J/ψ reconstructed at midrapidity. At low multiplicity density, $\langle p_T \rangle$ of prompt and non-prompt J/ψ from jetty events have a slight dominance in magnitude over the J/ψ produced from isotropic events. This is because the jetty events of the lowest multiplicity class are strongly dominated by the hard scatterings; the hadrons produced in such interactions have large transverse momenta, con-

sequently possessing a large value of $\langle p_T \rangle$ as compared to isotropic events in a similar multiplicity class. This difference is clearer in the case of midrapidity non-prompt J/ψ , the production source of which is primarily the initial hard scatterings. Here, at higher multiplicities ($\langle dN_{ch}/d\eta \rangle_{|\eta|<0.5} \gtrsim 12$), the distinction based on sphericity diminishes for non-prompt J/ψ while prompt J/ψ from isotropic events possess slightly higher $\langle p_T \rangle$ than their counterparts from jetty events. This indirectly signifies the role of MPI in charm hadron production in contrast to beauty hadrons. Further, one finds that the sphericity dependence of the $\langle p_T \rangle$ of prompt and non-prompt J/ψ is diminished at the forward rapidity.

The upper panels in Fig. 5 show the self-normalized yield of prompt and non-prompt J/ψ as a function of self-normalized charged particle multiplicity density at mid-pseudorapidity ($|\eta| < 0.5$), for S_0 -integrated, jetty and isotropic events in pp collisions at $\sqrt{s} = 13$ TeV using PYTHIA8. The left and right panels show the results at the mid and forward rapidities, respectively. The normalized J/ψ yield for both prompt and non-prompt cases increases with normalized charged particle density for measurements at both mid and forward rapidities and for all classes of transverse sphericity. However, in both the rapidity regions, for the S_0 -integrated case, one finds that the increment rate of non-prompt J/ψ is stronger as compared to the prompt case with an increase in self-normalized charged particle density. This is because the beauty hadrons are usually formed in initial hard scattering and are accompanied by high-energy jets, which can further fragment to produce hadrons, which can increase the charged particle multiplicity in the final state. Thus, the stronger-than-linear increase in non-prompt J/ψ production can be attributed to an autocorrelation bias [13]. As the particle multiplicity selection is performed in the forward rapidity region, one finds a com-

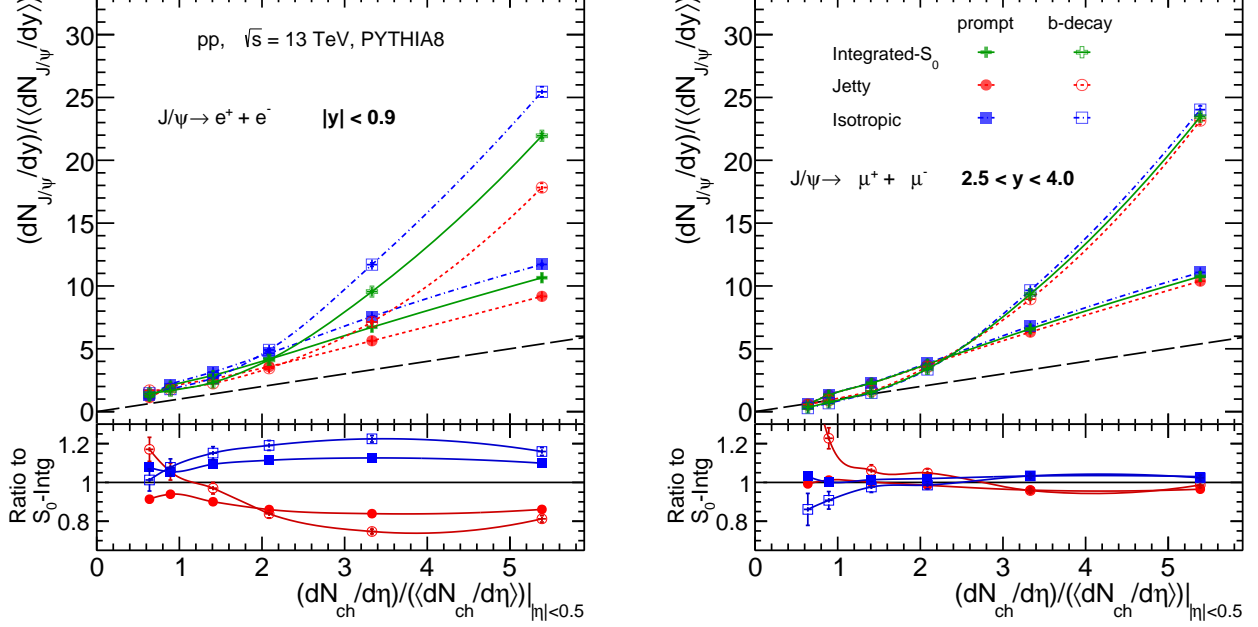


FIG. 5. (Color online) Normalized p_T -integrated prompt and non-prompt J/ψ yield as a function of normalized charged particle multiplicity density at midrapidity region ($|\eta| < 0.5$) with V0 multiplicity selection, for S_0 -integrated, jetty and isotropic events from pp collisions at $\sqrt{s} = 13$ TeV using PYTHIA8, for dielectron (left) and dimuon (right) production channels at $|y| < 0.9$ and $2.5 < y < 4$ rapidity ranges respectively. The dashed black line guides $(dN_{J/\psi}/dy)/((dN_{J/\psi}/dy)) = (dN_{ch}/d\eta)/((dN_{ch}/d\eta))$.

paratively smaller correlation bias than in the left panel, where both prompt and non-prompt J/ψ are measured in the midrapidity region, in contrast to the right panel, where the J/ψ is measured in the forward rapidity region.

Furthermore, the effect of this autocorrelation bias can be further explored with transverse sphericity. In Ref. [13], the effect of N_{mpi} is explored for both inclusive and non-prompt J/ψ . Here, the effects of N_{mpi} are similar to both inclusive and non-prompt J/ψ , except for extreme N_{mpi} events, where the yield of non-prompt J/ψ saturates. Interestingly, in the left panel of Fig. 5, we find that the yield of both prompt and non-prompt J/ψ is enhanced for the isotropic events having large N_{mpi} , while a lower self-normalized yield is observed for the jetty events with a small N_{mpi} value. This is a contradiction of the above-mentioned dependence of non-prompt J/ψ production with N_{mpi} , and can be attributed to self-correlation bias caused by measuring transverse sphericity in a similar rapidity region as the J/ψ . Although this bias is present in both prompt and non-prompt J/ψ measured at midrapidity, its production mechanism enhances the effects for the non-prompt case, which can be clearly visible in the lower left panel of Fig. 5. In contrast, the dependence of transverse sphericity is small on both prompt and non-prompt J/ψ measured at the forward rapidity, where the S_0 induced bias is small.

IV. SUMMARY

In this work, we study the transverse sphericity dependence of prompt and non-prompt J/ψ production in pp collisions at $\sqrt{s} = 13$ TeV using PYTHIA8. For the first time, the topological production of J/ψ is studied with an event shape. The study shows the effect of bias and the effects of MPI by studying the topological production of J/ψ in different pseudorapidity regions. We find that the non-prompt J/ψ possesses a harder transverse momentum spectrum as compared to the prompt J/ψ . The prompt J/ψ spectra are harder for the isotropic events as compared to the jetty events. The hardness of the p_T -spectra for the isotropic effects, which may arise as a consequence of multi-jet production environments and events with significantly large underlying event activity, in contrast to jetty events where the production of J/ψ is mostly dominated by di-jet like events, is noteworthy. This suggests that, although the J/ψ is produced in the initial stages, underlying MPI plays a crucial role in shaping the p_T -spectra. The effect extends to the beauty hadron production. A similar observation is made in Ref. [43] for $\Upsilon(nS)$ production.

Moreover, the non-prompt production fraction for the jetty events, dominated by the di-jet structure of particle production, increases with p_T and becomes higher than that of isotropic events. This identifies the dominance of the production of beauty hadron fraction in di-jet events in contrast to events with multi-jet environments. With

enough statistics in Run 3 of LHC data taking, this property of transverse sphericity can be exploited to study the production of charmonia in jets and offer valuable insights into the underlying hadronization mechanisms from pp to Pb–Pb collisions. This study provides a crucial understanding of charm and beauty hadron production through the study of prompt and non-prompt J/ψ with respect to different event shapes, including di-jet and multi-jet environments, where transverse sphericity acts as a probe.

Further, the self-normalized yield of J/ψ in the forward rapidity as a function of self-normalized charged particle multiplicity is affected by a higher autocorrelation bias as compared to the measurement of J/ψ in the midrapidity as the multiplicity selection is performed in the forward rapidity regions. In contrast, this autocorrelation bias is enhanced in the mid-rapidity region for transverse sphericity selection, which is defined in the mid-rapidity. This warns the scientific community to be careful while dealing with particle production at different rapidity regions and while making physics conclusions out of it.

ACKNOWLEDGEMENT

A.M.K.R. acknowledges the doctoral fellowships from the DST INSPIRE program of the Government of India. N.M. is supported by the Academy of Finland through the Center of Excellence in Quark Matter with Grant No. 346328. The authors gratefully acknowledge the DAE-DST, Government of India, funding under the mega-science project “Indian participation in the ALICE experiment at CERN” bearing Project No. SR/MF/PS-02/2021-IITI(E-37123).

APPENDIX

1. Comparison with experimental data

In Fig. 6, we compare the production cross-section of inclusive, prompt and non-prompt J/ψ from PYTHIA8 simulation of pp collisions at $\sqrt{s} = 13$ TeV with the corresponding data from ALICE [33, 44] and LHCb [45] for the midrapidity J/ψ (left plot) and forward rapidity J/ψ (right plot) respectively. Similar to the observation in Ref. [8] and consistent with Fig. 1, the production yield of J/ψ from b-hadron decays is almost 10 times lesser than the prompt J/ψ for the lower p_T values while this difference gets reduced at higher values of p_T . In the case of J/ψ reconstructed at midrapidity, the results from PYTHIA8 overestimate the experimental ALICE data. Thus, scaling factors of 0.1, 0.1, and 0.26 are applied respectively to the PYTHIA8 data of inclusive, prompt, and non-prompt J/ψ . Similarly, for the J/ψ measurements at forward rapidity, we multiply the PYTHIA8 results of inclusive and prompt J/ψ by 0.47 to match the

experimental data from LHCb. We see that the results from PYTHIA8 follow the experimental results fairly well till $p_T < 6$ TeV in both mid and forward rapidities, to deviate thereafter for the higher values of p_T .

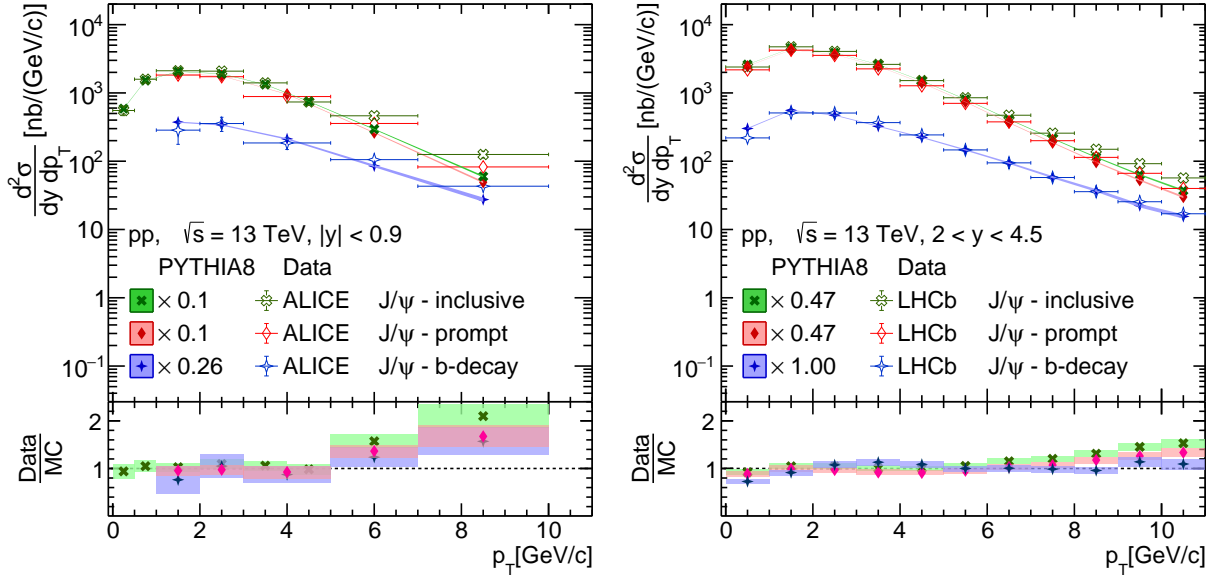


FIG. 6. (Color online) Comparison of inclusive, prompt and non-prompt J/ψ production cross-section from PYTHIA8 with ALICE data at midrapidity (left) and with LHCb data at forward rapidity (right) for pp collisions at $\sqrt{s} = 13$ TeV. The bottom panel shows the ratio of experimental data to the PYTHIA8 results.

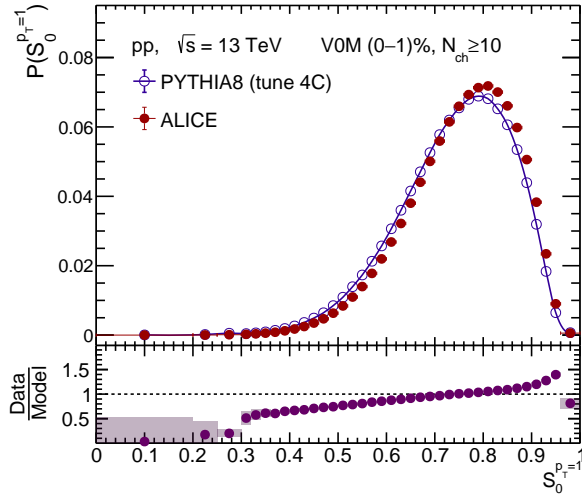


FIG. 7. Event normalized $S_0^{p_T=1}$ distribution for the 0–1% V0M multiplicity class for pp collisions at $\sqrt{s} = 13$ TeV from PYTHIA8 and the experimental data from ALICE [17] (upper panel). Ratio in the lower panel compares ALICE experimental data to PYTHIA8 results.

- [1] S. A. Bass, M. Gyulassy, H. Stoecker and W. Greiner, J. Phys. G **25**, R1 (1999).
 [2] J. C. Collins, D. E. Soper and G. F. Sterman, Adv. Ser. Direct. High Energy Phys. **5**, (1989).

- [3] N. Brambilla, S. Eidelman, B. K. Heltsley, *et al.* Eur. Phys. J. C **71**, 1534 (2011).
 [4] J. Adam *et al.* [ALICE Collaboration], JHEP **07**, 051 (2015).

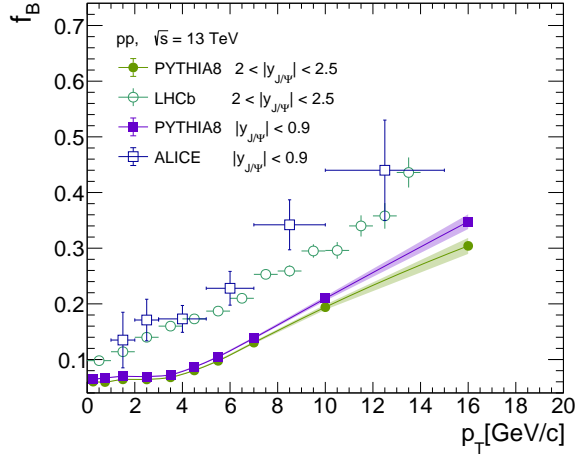


FIG. 8. Comparison of fraction of non-prompt J/ψ produced as a function of p_T for minimum-bias events from pp collisions at $\sqrt{s} = 13$ TeV from PYTHIA8 with ALICE (midrapidity) and LHCb (forward rapidity) data [33, 45].

- [5] S. Acharya *et al.* [ALICE Collaboration], *Eur. Phys. J. C* **78**, 466 (2018).
- [6] A. M. Sirunyan *et al.* [CMS Collaboration], *Eur. Phys. J. C* **77**, 269 (2017).
- [7] D. Acosta *et al.* [CDF Collaboration], *Phys. Rev. D* **71**, 032001 (2005).
- [8] S. Prasad, N. Mallick and R. Sahoo, *Phys. Rev. D* **109**, 014005 (2024).
- [9] B. Abelev *et al.* [ALICE Collaboration], *Phys. Lett. B* **712**, 165 (2012).
- [10] S. Acharya *et al.* [ALICE Collaboration], *Phys. Lett. B* **810**, 135758 (2020).
- [11] S. Acharya *et al.* [ALICE Collaboration], *JHEP* **06**, 015 (2022).
- [12] S. Acharya *et al.* [ALICE Collaboration], *JHEP* **07**, 238 (2025).
- [13] S. G. Weber, A. Dubla, A. Andronic and A. Morsch, *Eur. Phys. J. C* **79**, 36 (2019).
- [14] S. Prasad, S. Tripathy, B. Sahoo and R. Sahoo, [arXiv:2506.03782 [hep-ph]].
- [15] S. Prasad, B. Sahoo, S. Tripathy, N. Mallick and R. Sahoo, *Phys. Rev. C* **111**, 044902 (2025).
- [16] K. Goswami, S. Prasad, N. Mallick, R. Sahoo and G. B. Mohanty, *Phys. Rev. D* **110**, 034017 (2024).
- [17] S. Acharya *et al.* [ALICE Collaboration], *JHEP* **05**, 184 (2024).
- [18] J. Adam *et al.* [ALICE Collaboration], *JHEP* **09**, 148 (2015).
- [19] D. Thakur, S. De, R. Sahoo and S. Dansana, *Phys. Rev. D* **97**, 094002 (2018).
- [20] S. Deb, D. Thakur, S. De and R. Sahoo, *Eur. Phys. J. A* **56**, 134 (2020).
- [21] S. Prasad, N. Mallick, D. Behera, R. Sahoo and S. Tripathy, *Sci. Rep.* **12**, 3917 (2022).
- [22] S. Prasad, N. Mallick, S. Tripathy and R. Sahoo, *Phys. Rev. D* **107**, 074011 (2023).
- [23] S. Tripathy, S. Prasad and R. Sahoo, [arXiv:2504.09275 [nucl-ex]] (*Phys. Rev. D* (2025): In Press).
- [24] S. Prasad, A. M. Kavumpadikkal Radhakrishnan, R. Sahoo and N. Mallick, *Phys. Lett. B* **868**, 139753 (2025).
- [25] N. Mallick, R. Sahoo, S. Tripathy and A. Ortiz, *J. Phys. G* **48**, 045104 (2021).
- [26] N. Mallick, S. Tripathy and R. Sahoo, *Eur. Phys. J. C* **82**, 524 (2022).
- [27] A. Menon Kavumpadikkal Radhakrishnan, S. Prasad, S. Tripathy, N. Mallick and R. Sahoo, *Eur. Phys. J. Plus* **140**, 110 (2025).
- [28] S. Acharya *et al.* [ALICE Collaboration], *Eur. Phys. J. C* **79**, 857 (2019).
- [29] B. Andersson, G. Gustafson, G. Ingelman and T. Sjostrand, *Phys. Rept.* **97**, 31 (1983).
- [30] M. M. Aggarwal *et al.* [STAR Collaboration], *Phys. Rev. C* **84**, 034909 (2011).
- [31] R. Corke and T. Sjostrand, *JHEP* **03**, 032 (2011).
- [32] A. Banfi, G. P. Salam and G. Zanderighi, *JHEP* **06**, 038 (2010).
- [33] S. Acharya *et al.* [ALICE Collaboration], *JHEP* **03**, 190 (2022).
- [34] M. Aaboud *et al.* [ATLAS Collaboration], *Eur. Phys. J. C* **78**, 762 (2018).
- [35] V. Khachatryan *et al.* [CMS Collaboration], *Eur. Phys. J. C* **71**, 1575 (2011).
- [36] S. Acharya *et al.* [ALICE Collaboration], *Eur. Phys. J. C* **80**, 167 (2020).
- [37] Y. Bailung [ALICE Collaboration], *PoS LHCP2021*, 190 (2021).
- [38] Y. Bailung [ALICE Collaboration], *SciPost Phys. Proc.* **10**, 033 (2022).
- [39] S. Acharya *et al.* [ALICE Collaboration], *Phys. Lett. B* **843**, 137649 (2023).
- [40] S. Acharya *et al.* [ALICE Collaboration], *JHEP* **05**, 229 (2024).
- [41] A. Ortiz, A. Paz, J. D. Romo, S. Tripathy, E. A. Zepeda and I. Bautista, *Phys. Rev. D* **102**, 076014 (2020).
- [42] S. Acharya *et al.* [ALICE Collaboration], *Phys. Rev. C* **101**, 044907 (2020).
- [43] A. M. Sirunyan *et al.* [CMS Collaboration], *JHEP* **11**, 001 (2020).
- [44] S. Acharya *et al.* [ALICE Collaboration], *Eur. Phys. J. C* **81**, 1121 (2021).
- [45] R. Aaij *et al.* [LHCb Collaboration], *JHEP* **10**, 172 (2015).